

## Effect of Alumina Particle Size on Ni/Al<sub>2</sub>O<sub>3</sub> Catalysts for *p*-Nitrophenol Hydrogenation\*

CHEN Rizhi(陈立志)<sup>a</sup>, DU Yan(杜艳)<sup>b</sup>, XING Weihong(邢卫红)<sup>a</sup> and XU Nanping(徐南平)<sup>a,\*\*</sup>

<sup>a</sup> State Key Laboratory of Materials-Oriented Chemical Engineering, College of Chemistry and Chemical Engineering, Nanjing University of Technology, Nanjing 210009, China

<sup>b</sup> College of Environmental Sciences, Nanjing University of Technology, Nanjing 210009, China

**Abstract** The catalytic hydrogenation of *p*-nitrophenol to *p*-aminophenol was investigated over Ni/Al<sub>2</sub>O<sub>3</sub> catalyst on alumina support with different particle size. It is found that support particle size has significant influences on physiochemical properties and catalytic activity of the resulting Ni/Al<sub>2</sub>O<sub>3</sub> catalyst, but little influence on the selectivity. At a comparable amount of Ni loading, the catalytic activity of Ni/Al<sub>2</sub>O<sub>3</sub> prepared with alumina support of smaller particle size is lower. The reduction behavior of the catalyst is a key factor in determining the catalytic activity of Ni/Al<sub>2</sub>O<sub>3</sub> catalyst. The supported nickel catalyst 10.3Ni/Al<sub>2</sub>O<sub>3</sub>-3 improves the life span of the membrane by reducing fouling on the membrane surface compared to nano-sized nickel.

**Keywords** *p*-nitrophenol, catalytic hydrogenation, *p*-aminophenol, Ni/Al<sub>2</sub>O<sub>3</sub> catalysts, ceramic membrane filtration

### 1 INTRODUCTION

*p*-Aminophenol is of great commercial importance as an intermediate for the preparation of analgesic and antipyretic drugs[1—4]. In view of the growing demand for *p*-aminophenol, direct catalytic hydrogenation of *p*-nitrophenol to *p*-aminophenol becomes important, because this could be an efficient and greener route[5]. Up to now, some works have been reported on the liquid phase *p*-nitrophenol hydrogenation over Raney nickel[6], nano-sized nickel[7,8] and several noble metal catalysts such as Pt/C[5]. Our previous works have shown that the catalytic properties of nano-sized nickel have been proved to be superior to those of Raney nickel[8]. However, during the application of nano-sized nickel to membrane-based catalyst separation, it was found that nano-sized nickel particles would easily adsorb on the surface of pipeline, tank and membrane, which caused the decrease of catalyst concentration in reaction slurry and led to consequent decline in reaction rate and permeate flux of the membrane[9]. Due to their low cost and high catalytic activity, supported nickel catalysts are widely used in various reactions[10—13]. Moreover, compared to nano-sized nickel catalysts, the supported nickel catalysts are easy to be recovered by membrane separation process. More significantly, it is efficient to maintain high flux of membrane. So it is desired to find a supported nickel catalyst with better membrane filtration performance and comparable catalytic activity to replace nano-sized nickel. There are few reports on the catalytic hydrogenation of *p*-nitrophenol over supported nickel catalysts[14].

Therefore, this work is attempted to perform the catalytic hydrogenation of *p*-nitrophenol to *p*-aminophenol over Ni/Al<sub>2</sub>O<sub>3</sub> catalysts. The catalysts were prepared by liquid-phase chemical reduction method, and were

characterized by inductively coupled plasma (ICP), X-ray powder diffraction (XRD), X-ray photoelectron spectra (XPS) and temperature-programmed reduction (TPR) in order to correlate the catalytic activity with the characteristics of the catalysts. The effect of alumina support particle size on the physiochemical and catalytic properties of Ni/Al<sub>2</sub>O<sub>3</sub> catalysts was studied. At the same time, the membrane filtration performance of Ni/Al<sub>2</sub>O<sub>3</sub> suspension and nano-sized nickel suspension was compared.

### 2 EXPERIMENTAL

#### 2.1 Catalyst preparation

A series of Ni/Al<sub>2</sub>O<sub>3</sub> samples were prepared by a liquid-phase chemical reduction method. Nonporous Al<sub>2</sub>O<sub>3</sub> supports of three different mean particle sizes, *i.e.*, 1.3μm, 11.2μm, 22.8μm, measured by Mastersizer 2000 (Malvern, UK), were supplied by Zhengzhou Fuwei New Materials Co., China and designated as Al<sub>2</sub>O<sub>3</sub>-1, Al<sub>2</sub>O<sub>3</sub>-2, Al<sub>2</sub>O<sub>3</sub>-3, respectively. 10g of Al<sub>2</sub>O<sub>3</sub> calcined at 500°C for 4h in stagnant air was impregnated with 45ml of 0.42mol·L<sup>-1</sup> aqueous NiSO<sub>4</sub> solution for 8h under low magnetic stirring, was dried at 110°C under gentle stirring overnight to exclude residual water. 5g precursor was reduced by adding 8ml of hydrazine hydrate (N<sub>2</sub>H<sub>4</sub>·H<sub>2</sub>O) alkaline solution, during which the mole ratio of N<sub>2</sub>H<sub>4</sub>·H<sub>2</sub>O to Ni<sup>2+</sup> was controlled at 2:1 and the mixture was vigorously stirred. The resulting Ni/Al<sub>2</sub>O<sub>3</sub> catalyst was washed with deionized water at first, then by ethanol, and finally dried at 80°C in oven to get the black powders of supported nickel. The nickel content in all samples was analyzed by inductively coupled plasma (ICP, Optima 2000DV, PerkinElmer, USA) after extraction with nitric acid. The resulting catalysts were denoted as *x*Ni/support, where *x* is the actual nickel loading.

Received 2007-06-22, accepted 2007-09-23.

\* Supported by the Special Funds for Major State Basic Research Program of China (No.2003CB615702), the National Natural Science Foundation of China (No.20636020) and the Natural Science Foundation of Jiangsu Province (No.BK2006722).

\*\* To whom correspondence should be addressed. E-mail: npxu@njut.edu.cn

## 2.2 Catalyst characterization

X-ray powder diffraction (XRD) patterns of the catalysts were obtained on a Bruker D8 instrument with Ni-filtered Cu K $\alpha$  radiation ( $\lambda=0.154\text{nm}$ ) and operated at 40kV, 30mA and the scanning rate of  $0.05^\circ\cdot\text{s}^{-1}$  in the  $2\theta$  range from  $42^\circ$  to  $55^\circ$ .

X-ray photoelectron spectra (XPS) were obtained on an ESCALAB MK II system with a base pressure of  $1\times 10^{-4}\text{Pa}$ . Mg K $\alpha$  radiation source ( $h\nu=1253.6\text{eV}$ ) was used in the XPS measurements. The C<sub>1s</sub> signal (285eV) was taken as the reference to calculate the binding energies.

Temperature-programmed reduction (TPR) was carried out in a quartz U-tube reactor, and 100mg sample was used for each measurement. Prior to the reduction, the sample was pretreated in a N<sub>2</sub> stream at  $100^\circ\text{C}$  for 30min and then cooled down to room temperature. After that, the H<sub>2</sub>/Ar mixture (10% H<sub>2</sub> by volume) was switched on and the temperature was raised from  $30^\circ\text{C}$  to  $800^\circ\text{C}$  at a rate of  $10^\circ\text{C}\cdot\text{min}^{-1}$ . The consumption of H<sub>2</sub> in the reactant stream was detected by a thermal conductivity cell.

## 2.3 Hydrogenation experiment

The catalytic hydrogenation of *p*-nitrophenol to *p*-aminophenol was carried out in a 300ml stainless steel autoclave equipped with a magnetically driven impeller. After given amounts of one catalyst and 14g of *p*-nitrophenol in 163ml ethanol were introduced, the autoclave was sealed and purged with hydrogen five times to remove air; then, the reactor was heated to a desired temperature under low stirring ( $80\text{r}\cdot\text{min}^{-1}$ ), hydrogen gas was introduced into the reactor to a preset level, and the slurry were stirred at  $320\text{r}\cdot\text{min}^{-1}$ . The preliminary experiments proved that the hydrogenation reaction conducted at a stirring speed above  $300\text{r}\cdot\text{min}^{-1}$  is not influenced by external diffusion. Finally, the hydrogenation reaction was performed at  $102^\circ\text{C}$  and 1.65MPa. After the hydrogenation reaction was finished, the products were analyzed by a HPLC system (Agilent 1100 Series, USA) equipped with a diode array detector (DAD) and an auto-sampler. Chromatographic separations were performed at  $35^\circ\text{C}$  using a ZORBAX Eclipse XDB-C18,  $5\mu\text{m}$ ,  $4.6\text{mm}\times 250\text{mm}$  column. A mobile phase composed of 80% methanol and 20% water at a flow rate of  $1\text{ml}\cdot\text{min}^{-1}$  was used.

## 2.4 Membrane filtration experiment

In order to determine the membrane filtration behavior of the supported nickel catalyst, especially the effect of its presence on the permeate flux, the filtration performance of a nano-sized nickel catalyst suspension and a 10.3Ni/Al<sub>2</sub>O<sub>3</sub>-3 catalyst suspension with the same nickel concentration were performed. An asymmetric tubular ceramic membrane with 12mm outer diameter and 8mm inner diameter was used for the filtration experiments. The membrane was made up of a fine layer of  $\alpha$ -Al<sub>2</sub>O<sub>3</sub> with nominal pore size of  $0.5\mu\text{m}$  on the outwall of a tubular  $\alpha$ -Al<sub>2</sub>O<sub>3</sub> porous support, and was provided by Nanjing Jiusi High-Tech

Co., China. Nano-sized nickel particles with a mean size of 60nm were provided by Nanjing Jiusi High-Tech Co., China. During the filtration experiments the catalyst particles were suspended in deionized water by stirring. The filtration was continuously obtained by using a suction pump at a transmembrane pressure of 0.08MPa and a temperature of  $25^\circ\text{C}$ . After each run of experiments the membrane was cleaned with 10% (by volume) nitric acid and then rinsed with deionized water.

## 3 RESULTS AND DISCUSSION

### 3.1 Catalyst characterization

The XRD patterns of 10.3Ni/Al<sub>2</sub>O<sub>3</sub>-1, 9.8Ni/Al<sub>2</sub>O<sub>3</sub>-2, 10.3Ni/Al<sub>2</sub>O<sub>3</sub>-3 are shown in Fig.1. When alumina with small particle size is used as the support, no characteristic peaks of crystalline Ni can be observed, as shown in pattern (a). The result indicates that Ni is highly dispersed on the surface of Al<sub>2</sub>O<sub>3</sub>-1. For the samples that use Al<sub>2</sub>O<sub>3</sub>-2 and Al<sub>2</sub>O<sub>3</sub>-3 as supports and have a comparable Ni loading, however, the characteristic peak of crystalline Ni [ $2\theta=44.5^\circ$ , corresponding to the Miller index (111)] is observed, respectively, as shown in patterns (b) and (c) in Fig.1. Compared to 9.8Ni/Al<sub>2</sub>O<sub>3</sub>-2, 10.3Ni/Al<sub>2</sub>O<sub>3</sub>-3 shows a slightly sharper characteristic peak of crystalline Ni. These results show that alumina support particle size can greatly influence the dispersion of Ni loaded, and with catalysts using alumina of smaller size having the higher Ni dispersion. This is because alumina support of smaller size has higher specific surface area and thus provides more space for Ni deposition, resulting in better Ni dispersion.

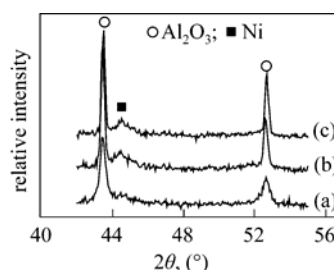


Figure 1 XRD patterns of the samples  
(a) 10.3Ni/Al<sub>2</sub>O<sub>3</sub>-1; (b) 9.8Ni/Al<sub>2</sub>O<sub>3</sub>-2; (c) 10.3Ni/Al<sub>2</sub>O<sub>3</sub>-3

The XPS results of 10.3Ni/Al<sub>2</sub>O<sub>3</sub>-1, 9.8Ni/Al<sub>2</sub>O<sub>3</sub>-2, 10.3Ni/Al<sub>2</sub>O<sub>3</sub>-3 are shown in Fig.2 and Table 1. The Ni<sub>2p</sub> spectra and the binding energies of Ni<sub>2p<sub>3/2</sub></sub> show that nickel on the surfaces of the three samples is oxidized completely[15], and no obvious difference exists in their Ni<sub>2p</sub> spectra. It is obvious from Table 1 that the surface Ni/Al atomic ratio increases with the increasing particle size of alumina support. This can be explained as follows: the ratio of alumina surface covered by Ni increases with increasing alumina support particle size, hence, the Ni atoms detected by XPS at certain surface area of alumina support increases with the increasing alumina support particle size, *viz.*, the surface Ni/Al atomic ratio for the sample using alumina of larger particle size as support is

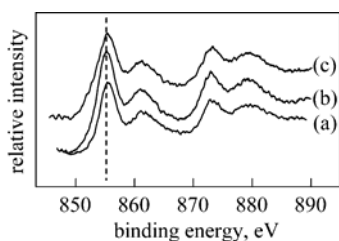


Figure 2 XPS spectra of Ni<sub>2p</sub> for the samples (a) 10.3Ni/Al<sub>2</sub>O<sub>3</sub>-1; (b) 9.8Ni/Al<sub>2</sub>O<sub>3</sub>-2; (c) 10.3Ni/Al<sub>2</sub>O<sub>3</sub>-3

Table 1 XPS results of surface elements of catalysts

Catalysts	Binding energy of Ni <sub>2p3/2</sub> , eV	Surface Ni/Al atomic ratio
10.3Ni/Al <sub>2</sub> O <sub>3</sub> -1	855.4	0.6
9.8Ni/Al <sub>2</sub> O <sub>3</sub> -2	855.3	1.3
10.3Ni/Al <sub>2</sub> O <sub>3</sub> -3	855.3	1.5

higher.

Figure 3 shows the TPR profiles of the samples. For the Al<sub>2</sub>O<sub>3</sub>-3, Al<sub>2</sub>O<sub>3</sub>-2 and Al<sub>2</sub>O<sub>3</sub>-1 samples, no obvious H<sub>2</sub> consumption can be observed at temperatures lower than 800°C, as shown in profiles (a), (b) and (c) in Fig. 3. The reduction profile of 10.3Ni/Al<sub>2</sub>O<sub>3</sub>-3 shows a broad hydrogen consumption band between 110°C and 600°C. The reduction at low temperature from 110°C to 260°C may be ascribed to the reduction of Ni<sub>2</sub>O<sub>3</sub>, which was also found by Hardiman *et al.*[16]. The reduction at high temperature is probably due to the reductions of bulk NiO and NiO with stronger interaction with the support[17]. The reduction peaks of 9.8Ni/Al<sub>2</sub>O<sub>3</sub>-2 and 10.3Ni/Al<sub>2</sub>O<sub>3</sub>-1 have profiles basically similar to those of 10.3Ni/Al<sub>2</sub>O<sub>3</sub>-3. However, it is interesting to note that the onset temperature and the temperature of maximum reduction ( $T_M$ ) obviously increase with the decreasing alumina support particle size. The results indicate that a stronger interaction between Ni and alumina support of smaller particle size exists, possibly due to the lower stacking height of nickel[18,19]. Comparing the profiles (d), (e) and (f), it is noted that the reduction peak areas are significantly different, and follow the order of 10.3Ni/Al<sub>2</sub>O<sub>3</sub>-1 > 9.8Ni/Al<sub>2</sub>O<sub>3</sub>-2 > 10.3Ni/Al<sub>2</sub>O<sub>3</sub>-3, signifying that the oxidation degree of Ni supported on alumina support of smaller particle size is comparatively higher. These results indicate that the re-

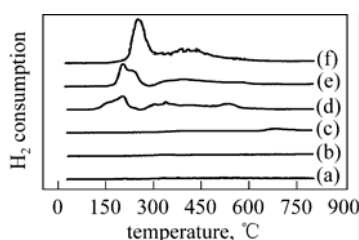


Figure 3 TPR profiles of the samples (a) Al<sub>2</sub>O<sub>3</sub>-3; (b) Al<sub>2</sub>O<sub>3</sub>-2; (c) Al<sub>2</sub>O<sub>3</sub>-1; (d) 10.3Ni/Al<sub>2</sub>O<sub>3</sub>-3; (e) 9.8Ni/Al<sub>2</sub>O<sub>3</sub>-2; (f) 10.3Ni/Al<sub>2</sub>O<sub>3</sub>-1

duction of nickel oxide to metallic nickel for the sample using alumina of smaller particle size as support is more difficult. Such discrepancies are also reflected in catalytic activities of these catalysts. The TPR results show the existence of nickel oxide on the surface of nickel, as also revealed by the XPS characterization.

### 3.2 Catalytic properties

The preliminary experiments on the hydrogenation of *p*-nitrophenol indicate that no hydrogenation reaction occurs in the absence of the catalyst, confirming the absence of any noncatalytic reaction. Moreover, at a fixed temperature, the partial pressure of solvent ethanol-water also remains constant. So, the decrease in the pressure in the reactor with time is caused only by catalytic hydrogenation of *p*-nitrophenol to *p*-aminophenol. Therefore, the catalytic activity could be expressed by the reaction rate defined as the amount of hydrogen consumed per minute and per gram nickel.

Figure 4 shows the catalytic activity (expressed as the reaction rates at 20min) of 10.3Ni/Al<sub>2</sub>O<sub>3</sub>-1, 9.8Ni/Al<sub>2</sub>O<sub>3</sub>-2, 10.3Ni/Al<sub>2</sub>O<sub>3</sub>-3 in the hydrogenation of *p*-nitrophenol to *p*-aminophenol, and for comparison purpose, the result of the nano-sized nickel catalyst with a mean particle size of 60nm is also presented. It can be found that compared to the nano-sized nickel catalyst, 10.3Ni/Al<sub>2</sub>O<sub>3</sub>-3 has higher catalytic activity, but the other two as-prepared Ni/Al<sub>2</sub>O<sub>3</sub> catalysts have lower ones. It is worth noting that the catalytic activities of the three alumina supported nickel catalysts are significantly different at a comparable Ni loading, and the catalytic activity order is as follows: 10.3Ni/Al<sub>2</sub>O<sub>3</sub>-1 < 9.8Ni/Al<sub>2</sub>O<sub>3</sub>-2 < 10.3Ni/Al<sub>2</sub>O<sub>3</sub>-3. The result clearly shows that the alumina support particle size has great influence on the catalytic activity of Ni/Al<sub>2</sub>O<sub>3</sub>. Together with the XRD characterization results mentioned above, it is interesting to find that the catalytic activity order of Ni/Al<sub>2</sub>O<sub>3</sub> is opposite to that of the nickel dispersion: the higher the nickel dispersion, the lower the catalytic activity. Combining these results with those of the TPR measurements as shown in Fig.3, it can be found

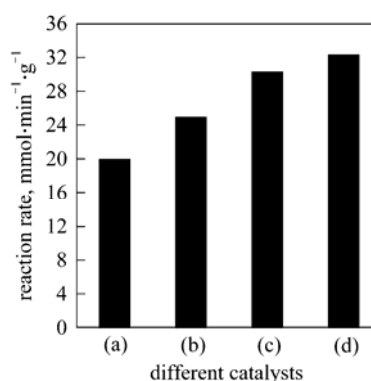


Figure 4 Reaction rate of *p*-nitrophenol hydrogenation over various catalysts

(a) 10.3Ni/Al<sub>2</sub>O<sub>3</sub>-1 (catalyst, 1.5g); (b) 9.8Ni/Al<sub>2</sub>O<sub>3</sub>-2 (catalyst, 1.5g); (c) nano-sized nickel (catalyst, 0.155g); (d) 10.3Ni/Al<sub>2</sub>O<sub>3</sub>-3 (catalyst, 1.5g)

that there is a very good correlation between the TPR data and the catalytic activity of Ni/Al<sub>2</sub>O<sub>3</sub>: the more difficult the reduction of nickel oxide to metallic nickel, the lower the catalytic activity. Therefore, one reasonable conclusion is that for the Ni/Al<sub>2</sub>O<sub>3</sub> using alumina of smaller particle size as support the reduction of nickel oxide to metallic nickel is more difficult under the similar reaction conditions, and as a result, the amounts of metallic nickel for this catalyst are few at a comparable Ni loading, and the corresponding catalytic activity is lower. Rode *et al.*[20] also found that the catalytic activity was higher for the supported nickel catalyst having a smaller degree of nickel dispersion in the gas-phase hydrogenation of benzonitrile and acetonitrile. They suggested that the surface geometry of nickel particles was of importance for the catalytic activity. According to these results, it is concluded that the reduction behavior of alumina supported nickel catalyst is a key factor in determining the catalytic activity of Ni/Al<sub>2</sub>O<sub>3</sub> in the hydrogenation of *p*-nitrophenol to *p*-aminophenol, and the catalytic activity is higher for the alumina supported nickel catalyst with an easier reduction of nickel oxide to metallic nickel.

The HPLC analysis results show that the contents of *p*-aminophenol in the products are all higher than 98% for the hydrogenation reactions catalyzed by Ni/Al<sub>2</sub>O<sub>3</sub> catalysts with three different particle size alumina supports, indicating that alumina support particle size has no influences on the catalytic selectivity of Ni/Al<sub>2</sub>O<sub>3</sub> in the hydrogenation reaction of *p*-nitrophenol.

### 3.3 Membrane filtration performance

Figure 5 shows the comparative results obtained with nano-sized nickel at 2.06g·L<sup>-1</sup> and 10.3Ni/Al<sub>2</sub>O<sub>3</sub>-3 at 20g·L<sup>-1</sup> during membrane filtration process. It is evident from the membrane performance that when 10.3Ni/Al<sub>2</sub>O<sub>3</sub>-3 is mixed with deionized water, the permeate flux is improved. For the nano-sized nickel suspension, the permeate flux is 527L·m<sup>-2</sup>·h<sup>-1</sup> at the filtration duration time of 200min while the permeate flux is 615L·m<sup>-2</sup>·h<sup>-1</sup> for the 10.3Ni/Al<sub>2</sub>O<sub>3</sub>-3 suspension. Clearly, the supported nickel catalyst 10.3Ni/Al<sub>2</sub>O<sub>3</sub>-3

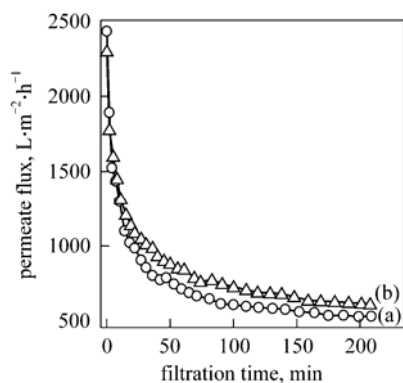


Figure 5 Change of permeate flux with filtration time

○ nano-sized nickel (catalyst, 2.06g·L<sup>-1</sup>);  
 △ 10.3Ni/Al<sub>2</sub>O<sub>3</sub>-3 (catalyst, 20g·L<sup>-1</sup>)

improves the life span of the membrane by reducing fouling on the membrane surface. Moreover, unlike nano-sized nickel the supported nickel particles will not easily deposit internally, which will not eventually cause membrane pores closure.

## 4 CONCLUSIONS

A series of Ni/Al<sub>2</sub>O<sub>3</sub> catalysts were prepared by a liquid-phase chemical reduction method, and characterized by ICP, XRD, XPS and TPR. The catalyst characterization results show that alumina support particle size has significant influences on the dispersion and reduction behavior of alumina supported nickel catalysts. The catalytic hydrogenation of *p*-nitrophenol to *p*-aminophenol was investigated over Ni/Al<sub>2</sub>O<sub>3</sub> catalysts in a laboratory-scale batch-slurry reactor. At a comparable amount of Ni loading, the catalytic activity of Ni/Al<sub>2</sub>O<sub>3</sub> using alumina of smaller particle size as support is lower under the similar reaction conditions. The reduction behavior of alumina supported nickel catalyst plays a key role in determining the catalytic activity of Ni/Al<sub>2</sub>O<sub>3</sub> in the hydrogenation of *p*-nitrophenol to *p*-aminophenol, and the catalytic activity is higher for the alumina supported nickel catalyst with an easier reduction of nickel oxide to metallic nickel. The high performance liquid chromatography (HPLC) analysis results show that alumina support particle size almost has no influences on the catalytic selectivity of Ni/Al<sub>2</sub>O<sub>3</sub> in the hydrogenation reaction of *p*-nitrophenol. According to the membrane filtration experiments, the permeate flux of membrane is improved and thus the membrane fouling phenomenon is reduced with the use of supported nickel catalyst 10.3Ni/Al<sub>2</sub>O<sub>3</sub>-3. Therefore, the 10.3Ni/Al<sub>2</sub>O<sub>3</sub>-3 catalyst can be potentially applied in the hydrogenation of *p*-nitrophenol to *p*-aminophenol.

## REFERENCES

- 1 Yun, K.S., Cho, B.W., "Process for preparing *para*-aminophenol", US Pat., 5066369 (1991).
- 2 Rode, C.V., Vaidya, M.J., Jaganathan, R., Chaudhari, R.V., "Hydrogenation of nitrobenzene to *p*-aminophenol in a four-phase reactor: Reaction kinetics and mass transfer effects", *Chem. Eng. Sci.*, **56**, 1299—1304(2001).
- 3 Rode, C.V., Vaidya, M.J., Chaudhari, R.V., "Synthesis of *p*-aminophenol by catalytic hydrogenation of nitrobenzene", *Org. Process Res. Dev.*, **3**, 465—470(1999).
- 4 Komatsu, T., Hirose, T., "Gas phase synthesis of *para*-aminophenol from nitrobenzene on Pt/zeolite catalysts", *Appl. Catal. A Gen.*, **276**, 95—102(2004).
- 5 Vaidya, M.J., Kulkarni, S.M., Chaudhari, R.V., "Synthesis of *p*-aminophenol by catalytic hydrogenation of *p*-nitrophenol", *Org. Process Res. Dev.*, **7**, 202—208(2003).
- 6 Chen, R.Z., Du, Y., Chen, C.L., Xing, W.H., Xu, N.P., Chen, C.X., Zhang, Z.L., "Comparative study on catalytic activity and stability of nano-sized nickel and Raney nickel", *J. Chem. Ind. Eng. (China)*, **54**, 704—706(2003). (in Chinese)
- 7 Du, Y., Chen, H.L., Chen, R.Z., Xu, N.P., "Poisoning effect of some nitrogen compounds on nano-sized nickel catalysts in *p*-nitrophenol hydrogenation", *Chem. Eng. J.*, **125**, 9—14(2006).
- 8 Du, Y., Chen, H.L., Chen, R.Z., Xu, N.P., "Synthesis of

- p*-aminophenol from *p*-nitrophenol over nano-sized nickel catalysts”, *Appl. Catal. A Gen.*, **277**, 259—264(2004).
- 9 Zhong, Z.X., Xing, W.H., Jin, W.Q., Xu, N.P., “Adhesion of nanosized nickel catalysts in the nanocatalysis/UF system”, *AIChE J.*, **53**, 1204—1210(2007).
  - 10 Rautanen, P.A., Aittamaa, J.R., Krause, A.O.I., “Liquid phase hydrogenation of tetralin on Ni/Al<sub>2</sub>O<sub>3</sub>”, *Chem. Eng. Sci.*, **56**, 1247—1254(2001).
  - 11 Toppinen, S., Rantakylä, T.K., Salmi, T., Aittamaa, J., “The liquid phase hydrogenation of benzene and substituted alkylbenzenes over a nickel catalyst in a semi-batch reactor”, *Catal. Today*, **38**, 23—30(1997).
  - 12 Quincoces, C.E., González, M.G., “Kinetic study on CO<sub>2</sub> reforming of methane”, *Chin. J. Chem. Eng.*, **9**, 190—195(2001).
  - 13 Kapoor, M.P., Matsumura, Y., “A comparative study of liquid- and gas-phase methanol decomposition catalyzed over nickel supported on silica”, *J. Mol. Catal. A Chem.*, **178**, 169—172(2002).
  - 14 Chen, R.Z., Du, Y., Xing, W.H., Xu, N.P., “The effect of titania structure on Ni/TiO<sub>2</sub> catalysts for *p*-nitrophenol hydrogenation”, *Chin. J. Chem. Eng.*, **14**, 665—669(2006).
  - 15 Zheng, H.G., Liang, J.H., Zeng, J.H., Qian, Y.T., “Preparation of nickel nanopowders in ethanol-water system (EWS)”, *Mater. Res. Bull.*, **36**, 947—952(2001).
  - 16 Hardiman, K.M., Hsu, C.H., Ying, T.T., Adesina, A.A., “The influence of impregnating pH on the postnatal and steam reforming characteristics of a Co-Ni/Al<sub>2</sub>O<sub>3</sub> catalyst”, *J. Mol. Catal. A Chem.*, **239**, 41—48(2005).
  - 17 Ho, S.W., Chu, C.Y., Chen, S.G., “Effect of thermal treatment on the nickel state and CO hydrogenation activity of titania-supported nickel catalysts”, *J. Catal.*, **178**, 34—48(1998).
  - 18 Wang, H., Fan, Y., Shi, G., Liu, Z.H., Liu, H.Y., Bao, X.J., “Highly dispersed NiW/ $\gamma$ -Al<sub>2</sub>O<sub>3</sub> catalyst prepared by hydrothermal deposition method”, *Catal. Today*, **125**, 149—154(2007).
  - 19 Wang, H., Fan, Y., Shi, G., Liu, H.Y., Bao, X.J., “Highly dispersed W/Al<sub>2</sub>O<sub>3</sub> hydrodesulfurization catalyst prepared by hydrothermal deposition method”, *Chin. J. Catal.*, **28**, 364—370(2007). (in Chinese)
  - 20 Rode, C.V., Arai, M., Shirai, M., Nishiyama, Y., “Gas-phase hydrogenation of nitriles by nickel on various supports”, *Appl. Catal. A Gen.*, **148**, 405—413(1997).